Journal of Environmental Management 157 (2015) 103–110

Contents lists available at ScienceDirect

Journal of Environmental Management

journal homepage: www.elsevier.com/locate/jenvman

Photocatalytic decomposition behavior and reaction pathway of sulfamethazine antibiotic using TiO_2

Shuji Fukahori [a, c, *], Taku Fujiwara [b, c]

[a] Center for Paper Industry Innovation, Ehime University, 127 Mendoricho Otsu, Shikokuchuo, Ehime 799-0113, Japan
[b] Research and Education Faculty, Natural Sciences Cluster, Agriculture Unit, Kochi University, 200 Monobe Otsu, Nankoku, Kochi 783-8502, Japan
[c] Japan Science and Technology Agency, CREST, Japan

ARTICLE INFO

Article history:
Received 13 February 2015
Received in revised form
29 March 2015
Accepted 1 April 2015
Available online 17 April 2015

Keywords:
Sulfonamide
Antibiotics
Photocatalytic decomposition
TiO_2
Intermediate product

ABSTRACT

The photocatalytic degradation of sulfanethazine (SMT), one of the sulfonamide antibiotics, in aqueous solution by TiO_2 was investigated. The time courses of SMT concentration, the amount of non-purgeable organic carbon, and the concentrations of ions such as SO_4^{2-}, NH_4^+, and NO_3^- formed during the photocatalytic reaction were measured and the structures of seven intermediates formed with the disappearance of SMT were also estimated by LC/MS/MS analyses. In addition to that of SMT, the decomposition behaviors of model compounds sulfanilic acid (SA) and 4-amino-2, 6-dimethylpyrimidine (ADMP) were investigated using the TiO_2/UV system. The observed photocatalytic degradation behaviors of SMT, SA, and ADMP gave new insight into the degradation pathway of SMT. Especially, the formation of *p*-aminophenol during SMT decomposition, which until now has not been reported in previous studies concerning the photocatalytic decomposition of SMT and other sulfonamide antibiotics. These results indicate the existence of a novel photocatalytic degradation pathway for sulfonamides. The direct substitution of the sulfonamide group with a hydroxyl group is suggested.

1. Introduction

Synthetic antimicrobial agents are widely used to prevent infection in humans and livestock. However, many pharmaceuticals are not fully metabolized in human or livestock bodies and are excreted in urine or feces. A number of pharmaceuticals are increasingly found in the environment, which poses a serious problem because they cannot be removed through conventional wastewater treatment (Hernando et al., 2006). Although the concentration of pharmaceuticals detected in natural water or effluent from sewage treatment plants is quite low (ng/L–μg/L), the ecotoxicity of pharmaceuticals at μg/L levels has been reported (Fent et al., 2006). Suitable treatment methods for the removal of discharged pharmaceuticals are required for the sustainable and safe use of water in the future, and research on water purification methods is currently being conducted in scientific and industrial circles (Ternes et al., 2003; Kim et al., 2009).

Sulfonamide antibiotics, which have a sulfanilamide structure, are widely used as food additives in livestock production (Committee on Drug Use in Food Animals 1999) and are commonly detected in natural water or secondary effluent (Heberer, 2002; Bendz et al., 2005). Some researchers have already reported the advanced oxidation of sulfonamide antibiotics (Kaniou et al., 2005; Abellán et al., 2007; Hu et al., 2007; Baran et al., 2009; Yang et al., 2010). For example, Baran et al. investigated the photocatalytic degradation of sulfonamides with TiO_2, Fe salts, and TiO_2/$FeCl_3$ (Baran et al., 2009). They reported a relationship between the experimental conditions and degradation efficiency and the intermediate products detected. Yang et al. described the photocatalytic degradation kinetics and mechanism of sulfonamide antibiotics using TiO_2 (Yang et al., 2010). Although they measured the formation of inorganic ions such as SO_4^{2-} and NH_4^+, the degradation mechanism was not given. Hu et al. investigated the active mechanism responsible for photocatalytic degradation of sulfamethoxazole by systematically examining the influence of pH, dissolved oxygen, organic contaminants, and ions on the reaction kinetics (Hu et al., 2007). They also detected some degradation intermediates and deduced the degradation pathway; however, only three intermediates were detected and the discussion of the

* Corresponding author. Center for Paper Industry Innovation, Ehime University, 127 Mendoricho Otsu, Shikokuchuo, Ehime 799-0113, Japan.
E-mail addresses: fukahori.shuji.mj@ehime-u.ac.jp (S. Fukahori), fujiwarat@kochi-u.ac.jp (T. Fujiwara).

http://dx.doi.org/10.1016/j.jenvman.2015.04.002

degradation mechanism was not sufficient.

The effects of reaction conditions such as TiO_2 concentration, pH, UV intensity, and organic contaminants on the reaction rate of sulfonamide antibiotic degradation have already been revealed in our previous studies (Fukahori et al., 2012; Ito et al., 2013). We also suggested the degradation behavior of crotamiton, an antipruritic that is often detected in Japanese rivers, based on the detection of intermediates and ions over time using LC/MS/MS and ion chromatography. In the present study, we detected or deduced the major intermediates formed during the photocatalytic decomposition of SMT and its analogues, and investigated their degradation behaviors. One of the detected intermediates has not previously been reported for the photocatalytic decomposition of sulfonamide antibiotics, indicating the discovery of a novel photocatalytic degradation pathway.

2. Experimental

2.1. Chemicals

TiO_2 powder (P-25, 50 m^2/g, anatase; Degussa, Dusseldorf, Germany) was obtained commercially. SMT (purity 99%) was purchased from Aldrich, sulfanilic acid (SA, 99%), sulfanilamide (SAm, 99.7%), 4-amino-2, 6-dimethylpyrimidine (ADMP, 97%), *o*-aminopheno (*o*-AP, 97%), *m*-aminophenol (*m*-AP, 98%) and *p*-aminophenol (*p*-AP, 98%) were purchased from Wako Pure Chemical Industries, Ltd (Osaka, Japan). The molecular structures of the pharmaceuticals are given in Fig. 1. All chemicals were of reagent grade. All other reagents, including acetonitrile, sulfuric acid, sodium hydroxide and formic acid, were used without further purification.

2.2. Photocatalytic decomposition using TiO_2

The pharmaceutical sample solution (10 mg/L, 50 mL) was prepared using Millipore water (Millipore, Billerica, MA, USA) and poured into a glass vessel. TiO_2 powder was added to the reaction vessel (0.2 g/L). The pH was adjusted to 7 using sulfuric acid or sodium hydroxide with measurement by a portable pH meter (D-51; Horiba, Kyoto, Japan). The solution was stirred at 25 °C and irradiated with a UV lamp (UV intensity, 1 mW/cm^2). The effect of pH and TiO_2 concentration on the photocatalytic decomposition were investigated in our previous study (Fukahori et al., 2012). After UV irradiation, a designated aliquot was filtered with a membrane filter (DISMIC, pore size: 0.2 μm; ADVANTEC, Tokyo, Japan) and subjected to ultra performance liquid chromatography-tandem mass spectrometry (LC/MS/MS, ACQUITY UPLC-Xevo TQ; Waters, Milford, MA, USA). C and C_0 are the concentration of target compound such as SMT, SA and ADMP at time 0 and t, respectively.

2.3. Quantitative analyses

The LC/MS/MS analysis was carried out using a BEH C18 column (2.1 × 150 mm; Waters) with a linear gradient from 10% acetonitrile in 0.05% formic acid (isocratic for 0.5 min) to 90% (0.5–7 min) at a constant flow rate of 0.3 mL/min. A photodiode array detector (PDA) was placed between the analytical column and the MS/MS, and the wavelength was set at 254 nm. In order to confirm the

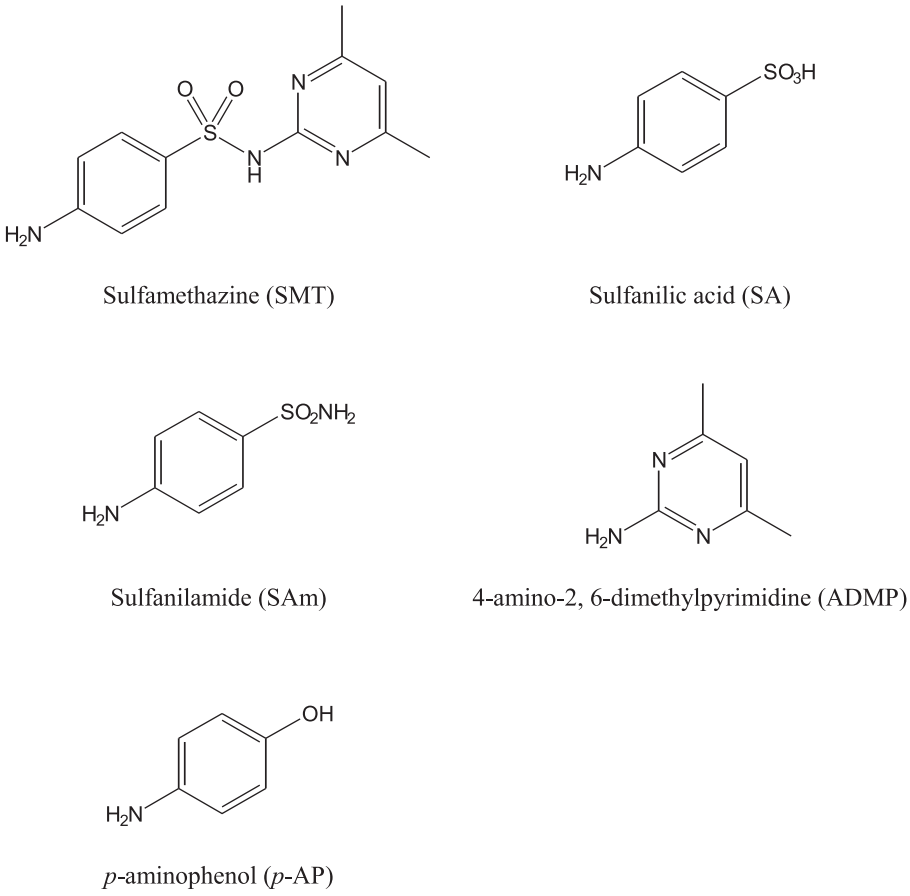

Fig. 1. Structures of chemicals used.

accuracy of UPLC analysis, the standard samples were measured three times and we confirmed the coefficient of variance of peak area was <5%. The structures of the intermediates were determined or deduced through comparison with standards or interpretation of the mass patterns obtained by LC/MS/MS.

The non-purgeable organic carbon (NPOC, mg-C/L) content in the treated water was measured using a Shimadzu TOC analyzer (TOC-5000A) based on CO_2 quantification by non-dispersive infrared analysis after high temperature catalytic combustion. *NPOC* and $NPOC_0$ are the content of NPOC at time 0 and t, respectively. The concentrations of NH_4^+, NO_3^-, and SO_4^{2-} in the treated water were measured using ion chromatography (DX-120; Dionex, Sunnyvale, CA, USA). The NH_4^+ concentration was measured using a CS12A column (4 × 250 mm; Dionex) with 19.8 mM methanesulphonic acid as the eluent (flow rate 1 mL/min). The NO_3^- and SO_4^{2-} concentrations were analyzed using an AS12A anionic column (4 × 200 mm; Dionex) and a mixture of 2.7 mM Na_2CO_3 and 0.3 mM $NaHCO_3$ (flow rate 1.5 mL/min).

3. Results and discussion

3.1. Photocatalytic decomposition of SMT using TiO_2

The time courses of SMT concentration and NPOC content measured during the photocatalytic decomposition of SMT are shown in Fig. 2a. After 2 h UV irradiation, ca. 95% of the SMT had been decomposed, whereas only 60% of the TOC had been removed. It took 24 h to mineralize all of the SMT, indicating that the SMT was converted to intermediates and that much of these remained until 24 h. The amount of NPOC decreased smoothly until 3 h, after which the rate of decrease was low.

To confirm the mineralization of SMT, we also measured the concentrations of ions in the reaction mixture. It has been reported that nitrogen and sulfur atoms are converted to NH_4^+, NO_3^-, and SO_4^{2-} during the photocatalytic decomposition of organic compounds by TiO_2. Although the formation of such ions during the photocatalytic decomposition of sulfonamide antibiotics has been reported, the details were not discussed (Kaniou et al., 2005; Abellán et al., 2007; Hu et al., 2007; Baran et al., 2009; Yang et al., 2010). The time courses of ion formation during the photocatalytic treatment of SMT are shown in Fig. 2b. For an initial SMT concentration of 10 mg/L, the maximum inorganic nitrogen and sulfur concentrations expected if all the SMT was mineralized were 2.01 mg-N/L and 1.15 mg-S/L, respectively. The NH_4^+ and SO_4^{2-} concentrations increased immediately and leveled off after 24 and 12 h treatment, respectively. Baran et al. and Yang et al. reported the cleavage of sulfonamide bond and suggested the formation of sulfanilic acid as an intermediate (Baran et al., 2009; Yang et al., 2010). In this study, the stoichiometric amount of SO_4^{2-} evolved (ca. 1.1 mg-S/L) after 24 h treatment indicated that the cleavage of sulfonamide occurred as the initial step.

On the other hand, the concentration of NH_4^+-N after 96 h treatment was ca. 1.0 mg-N/L, half of the stoichiometric amount. The concentration of NO_3^- gradually increased and reached 0.8 mg-N/L after 96 h treatment. The total nitrogen derived from NH_4^+ and NO_3^- was 1.8 mg-N/L, indicating that almost all of the nitrogen in SMT was mineralized by the photocatalytic treatment.

3.2. Intermediates formed during the photocatalytic decomposition of SMT

To estimate the degradation pathway of SMT, the intermediates formed through the photocatalytic decomposition of SMT were measured using mass spectrometry. Full-scan and selective ion recording (SIR) mode LC/MS/MS revealed the formation of new

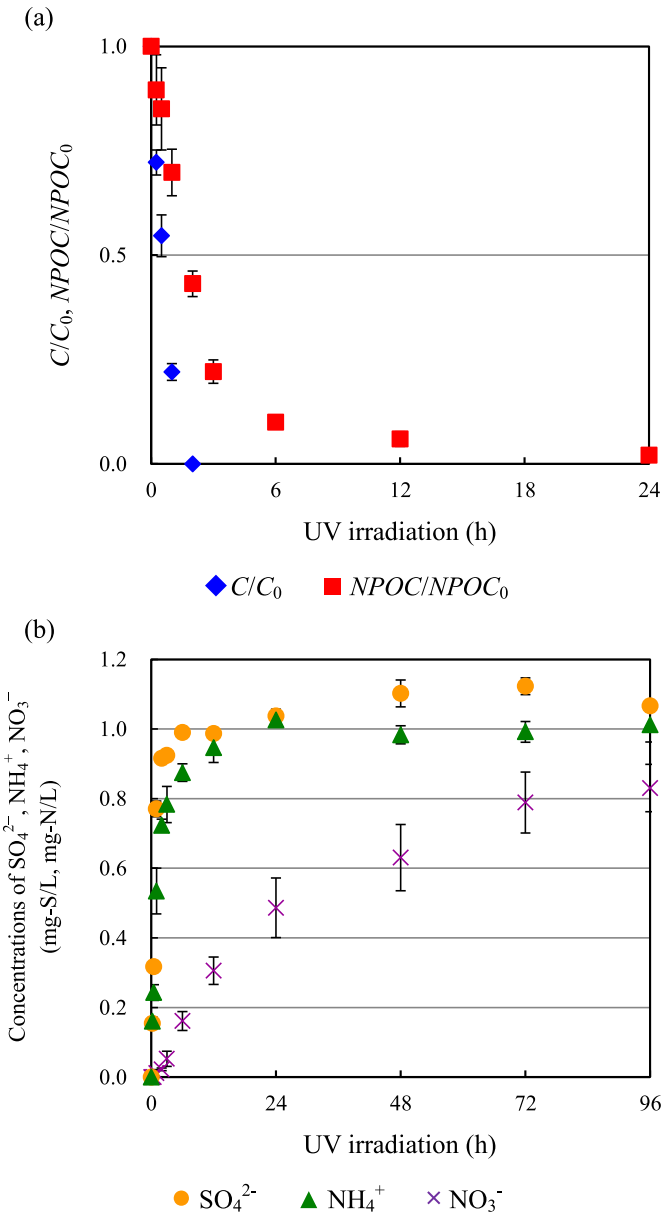

Fig. 2. Photocatalytic decomposition behavior of SMT. Changes in concentrations of SMT and NPOC content (a) and ions formed (b) during the degradation of SMT.

peaks concurrent with the disappearance of SMT. Fig. 3 depicts the product ion spectra of SMT and major intermediates. The ordinate shows the ratio of detected intensity of fragment ions to that of base peak ion. The data presented in Fig. 3 were obtained under optimized collision energy and cone voltage, determined in electrospray ionization (ESI)-MS/MS experiments on an Xevo-TQ instrument. The fragmentation pattern of SMT (Fig. 3a) gave us the information needed to deduce several substituents and identify the unknown intermediates. The most characteristic signals were *m*/*z* 213, 204, 186, 156, 124, 108, and 92 fragments. The deduced structures of the fragment ions are shown in Fig. 3. The fragment ions 156 and 124 were derived from the amino phenyl and pyrimidinyl portions, respectively, formed through cleavage of the sulfonamide group. The loss of SO from fragment ion *m*/*z* 156 gave the *m*/*z* 108 fragment ion, which by further loss of oxygen gave the anilinium ion (*m*/*z* 92). The fragment ion *m*/*z* 213 was attributed to $[M + H^+ - H_2SO_2]^+$. Furthermore, the cleavage of the C–S bond between

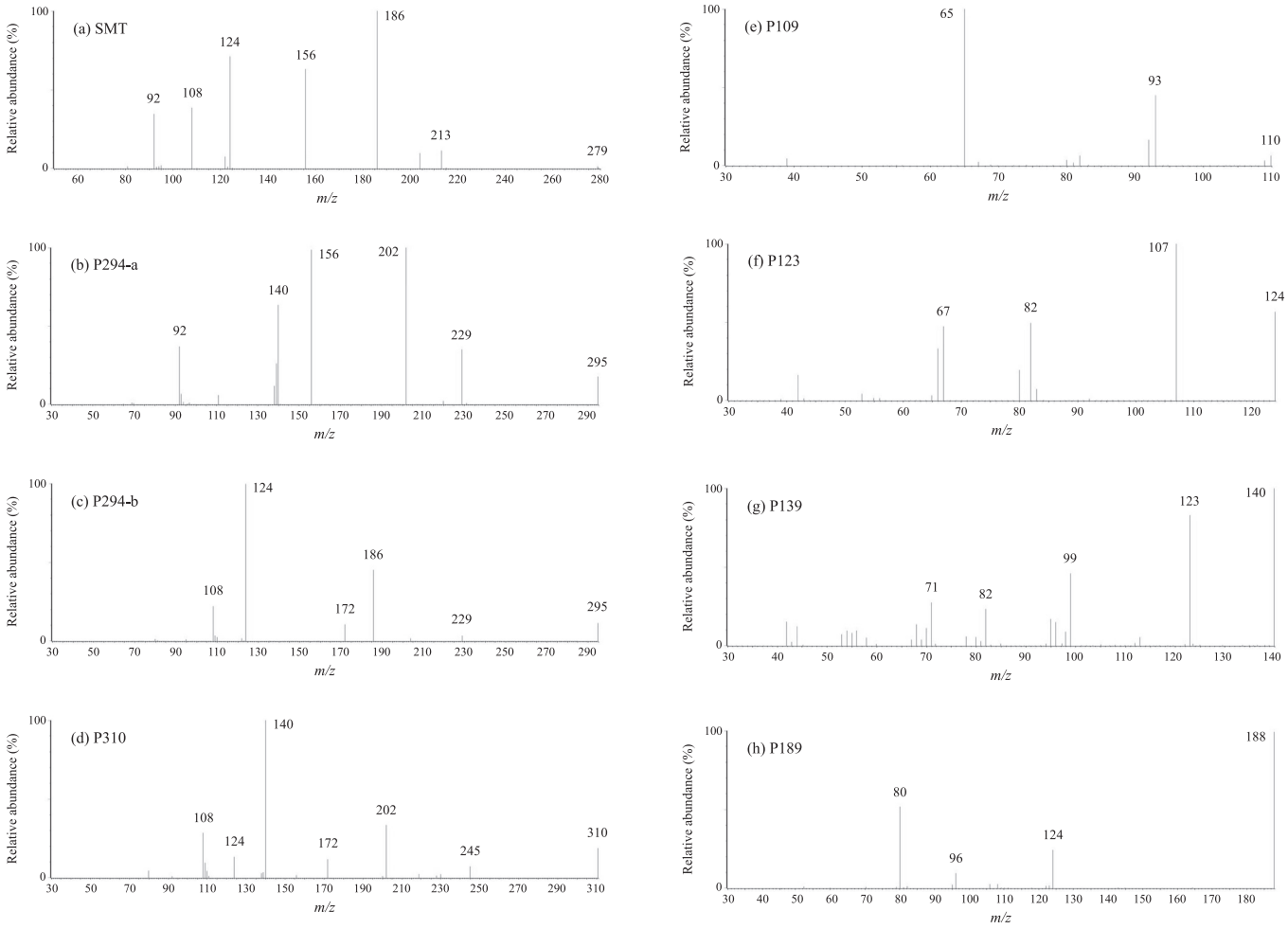

Fig. 3. Product ion spectra of SMT (a) and major intermediates: P294-a (b), P294-b (c), P310 (d), P109 (e), P123 (f), P139 (g), and P189 (h).

phenyl and sulfonamide gave the fragment *m*/*z* 186. In brief, the fragment ions 156, 108, and 92, and 186 and 124 were derived from phenyl and pyrimidinyl moieties, respectively.

The structures of seven types of intermediates were deduced from their estimated molecular weight and fragment pattern. At the initial stage of the photocatalytic decomposition of SMT, there were two noticeable peaks with molecular weight of 294, 16-Da larger than that of SMT (Fig. 3b, c, labeled as P294-a and P294-b, respectively). Previous studies have reported that the photocatalytic reaction proceeds mainly because of the electrophilic hydroxyl radicals produced through the oxidation of water molecules, and hydroxylation often occurs, resulting in a molecular weight increase of 16-Da (Fukahori et al., 2003; Hu et al., 2007; Yang et al., 2010; Fukahori et al., 2012). Thus, these two intermediates were expected to be hydroxylated analogs of SMT. However, the fragmentation patterns were quite different. The abundant fragments of P294-a (Pry-OH) were 229, 202, 156, 140, 111, and 92. The existence of the fragment ions *m*/*z* 156 and 92 indicates that the phenyl portion of SMT was unchanged, although fragment ions derived from the pyrimidinyl portion (*m*/*z* 186, 124) were not observed. Instead, the formation of fragment ions *m*/*z* 202 and 140 suggests the hydroxylation of the pyrimidinyl moiety of SMT. In contrast, the abundant fragments of P294-b (Ph-OH) were 186, 172, 124, and 108. The detection of fragment ions *m*/*z* 186 and 124 indicates that the pyrimidinyl moiety in SMT was preserved. The disappearance of the characteristic fragments of the amino phenyl portion (*m*/*z* 156, 108, and 92) strongly suggested the modification of the phenyl portion. We concluded that the fragment ions *m*/*z* 172, 124 and 108 were formed by the addition of oxygen atoms to the amino phenyl moiety.

The intermediate with larger molecular weight than P294 was P310 (Fig. 3d). The abundant fragments of P310 were 245, 202, 172, 140, 124, and 108. The fragment ions *m*/*z* 202 and 172 were judged to be hydroxylated phenyl and pyrimidinyl moieties, generated from the modification of fragment ions *m*/*z* 186 and 156 observed in the fragmentation of SMT. From this point of view, *m*/*z* 172, 124, 108 and 202, 140 were the fragment ions derived from hydroxylated phenyl and pyrimidinyl moieties. The fragment ion *m*/*z* 245 was attributed to $[M + H^+\text{-}H_2SO_2]^+$.

In the case of intermediates with smaller molecular weight than SMT, we detected compounds with *m*/*z* 109, 123, 139, and 189 (labeled as P109, P123, P140, and P189 in Fig. 3d, e, f, and g, respectively). P109, P123, and P139 were detected in positive and negative scan modes, respectively. From the molecular weight, we deduced P123 to be ADMP because previous researchers have reported the cleavage of the sulfonamide bond in SMT during photocatalytic treatment. Comparison of the UPLC retention time and fragmentation pattern of the fragment to those of standard ADMP confirmed that P123 was ADMP. Similarly, the characteristic fragment $[M+H]^+$-17 (*m*/*z* 123) was found in the mass spectrum of P139 (Fig. 3f), and was presumably a result of the detachment of NH_3. Based on the finding that ADMP had formed, P139 was

deduced to be hydroxylated ADMP (ADMP-OH). P189 was expected to have a sulfo group because it was detected in the negative scan mode, and the characteristic fragment ion $[M+H]^+$-64 forms through the detachment of SO_2. Based on its molecular weight, we deduced P189 to be hydroxylated SA (SA-OH).

For P109, the fragment ions $[M+H]^+$-17 (m/z 93) and $[M+H]^+$-17-28 (m/z 65) were observed. We concluded that the loss of the amine moiety from parent ion m/z 110 gave the m/z 93 fragment ion, which by further loss of C_2H_4 gave the m/z 65 ion. We deduced that P109 was AP, Comparison of the retention time and fragment patterns of *o*-, *m*- and *p*-AP with those of P109 revealed that P109 matched *p*-AP. Although no researchers have previously reported the formation of *p*-AP during the photocatalytic decomposition of sulfonamides, it was detected during the photocatalytic decomposition of SA in the present experiments.

The formation of SA or SAm during the photocatalytic decomposition of sulfonamide antibiotics was reported in some previous studies (Hu et al., 2007; Baran et al., 2009; Yang et al., 2010). However, in this study, these species were under the detectable limit of LC/MS/MS during the treatment of SMT, although we surveyed them using standard chemicals.

3.3. Photocatalytic decomposition of SA and ADMP

To investigate the photocatalytic decomposition behavior of SMT, model compounds were treated with TiO_2/UV. SA and ADMP were selected because the cleavage of sulfonamide was indicated. The time courses of SA or ADMP concentration and the concentrations of NPOC and ions during the photocatalytic treatment of SA and ADMP are shown in Figs. 4 and 5. During the treatment of SA, the SA concentration decreased quickly and reached below the detectable limit after 2 h treatment. The concentration of NPOC decreased gradually, but the rate was low at the initial stage. For the ions, NH_4^+ was the main nitrogen species detected and it was confirmed that the sulfo and amino groups attached to the aromatic ring were converted to SO_4^{2-} and NH_4^+ through photocatalytic decomposition. The SO_4^{2-} and NH_4^+ concentrations increased soon after UV irradiation started and reached stoichiometric amounts after 3 h treatment (0.81 mg-N/L and 1.85 mg-S/L, respectively). These results seemed to indicate modification of the aromatic ring or detachment of nitrogen or sulfur at the initial stage and subsequent mineralization of carbon.

In contrast, the mineralization of ADMP took longer than that of SA. Although the ADMP concentration was below the detectable limit after 2 h treatment, some organic species remained after 24 h. NO_3^- was also detected during ADMP decomposition, and the molar ratio of NO_3^- to NH_4^+ was ca. 2: 1. Vulliet et al. studied the photocatalytic treatment of *s*-triazine, a nitrogen-containing aromatic compound, and reported the formation of NO_3^- (Vulliet et al., 2002). Therefore, the two nitrogen atoms contained in the pyrimidine ring were converted to NO_3^- and the one nitrogen of the amino group was converted to NH_4^+. In addition, they also reported that it took a long time to mineralize *s*-triazine because it was converted to highly stable cyanuric acid. Aromatic compounds containing nitrogen in the aromatic ring are tolerant to photocatalytic decomposition. Thus, ADMP may have been converted to a stable compound similar to cyanuric acid, resulting in a longer treatment time.

The intermediates formed during the photocatalytic treatment of SA and ADMP were also investigated by LC/MS/MS. P189 and P139 were detected as main intermediates during the decomposition of SA and ADMP, respectively. These results support our deduction that P189 and P139 are SA-OH and ADMP-OH. Furthermore, P109 was also detected as an intermediate of SA degradation.

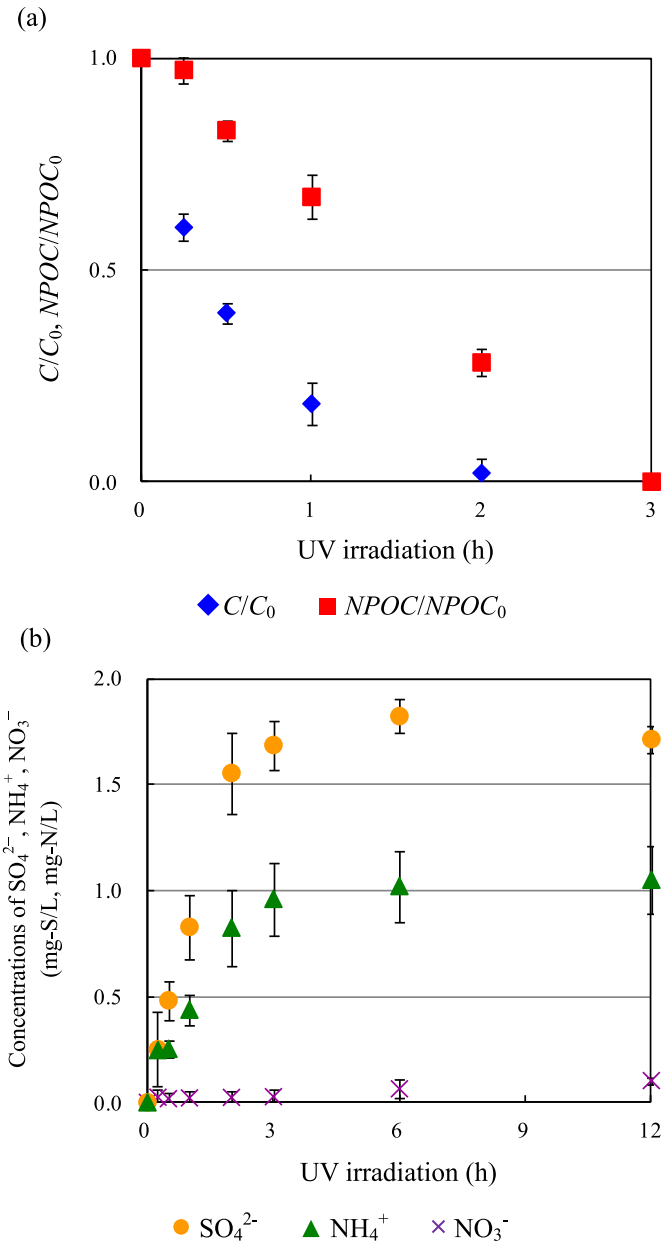

Fig. 4. Photocatalytic decomposition behavior of SA. Changes in concentrations of SA and NPOC content (a) and ions formed (b) during the degradation of SA.

3.4. Proposed degradation pathway for SMT

Fig. 6 shows the time course of P_t/P_{max} of the intermediates observed during the photocatalytic decomposition of SMT, where P_t is the intermediate peak area measured in SIR mode at treatment time t and P_{max} is the maximum peak area of each intermediate observed during the photocatalytic treatment. At the initial stage of SMT decomposition, hydroxylated SMT (Ph-OH and Pyr-OH) and *p*-AP were detected (Fig. 6). After their formation, further hydroxylated compounds (SMT-2OH), ADMP and SA-OH were detected, and finally ADMP-OH accumulated. From these results, we can suggest three initial reactions, beginning with 1. hydroxylation of the phenyl, 2. hydroxylation pyrimidine ring and 3. direct substitution of the sulfonamide group with a hydroxyl group. The proposed degradation pathway of SMT is shown as Fig. 7. These first two reactions are often observed in the photocatalytic decomposition of

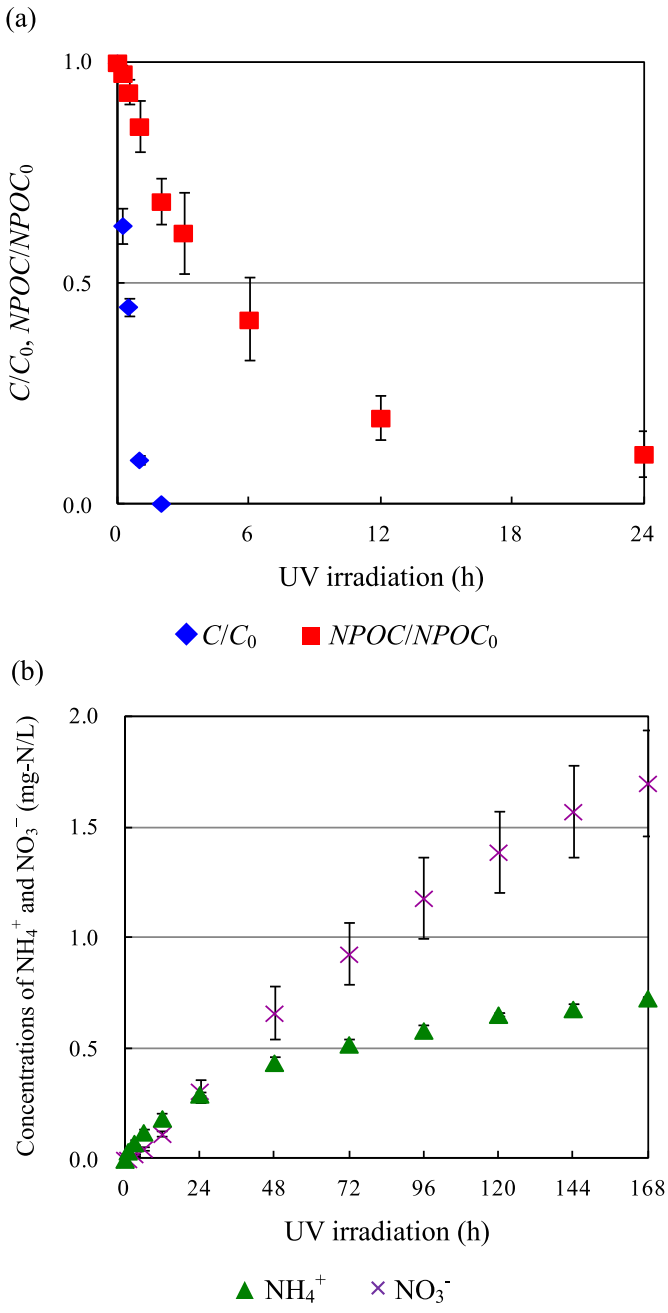

Fig. 5. Photocatalytic decomposition behavior of ADMP: Changes in concentrations of SA and NPOC content (a) and ions formed (b) during the degradation of ADMP.

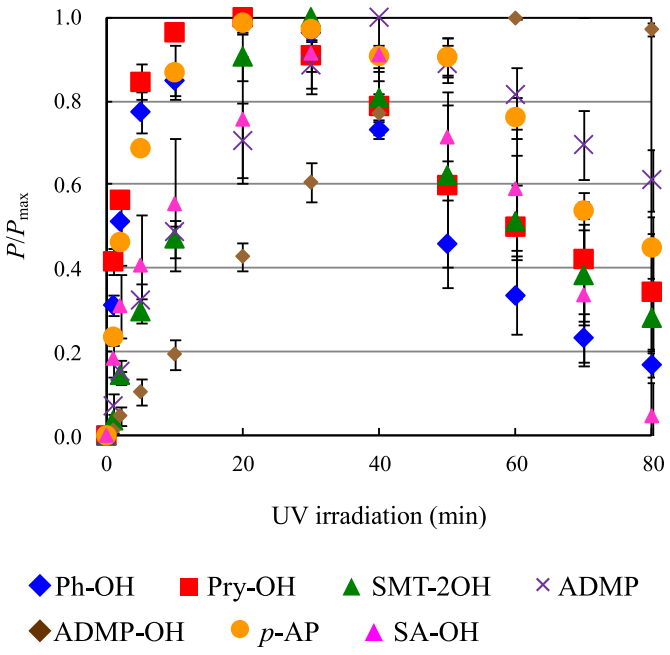

Fig. 6. Time courses of major intermediates.

aromatic compounds (Hu et al., 2007; Fukahori et al., 2012). Then, the S–N bond of sulfonamide group was broken, resulting in the formation of SA-OH and ADMP. SA-OH and ADMP-OH also form through the decomposition of SMT-2OH. Some researchers have reported that the cleavage of the sulfonamide group S–N bond occurs before the modification of the phenyl ring (Hu et al., 2007; Baran et al., 2009; Yang et al., 2010). However, the non-detection of SA and late formation of ADMP compared with that of hydroxylated SMT strongly supported that little direct cleavage of the S–N bond occurred. In addition, the non-detection of SAm or its derivatives also indicates that no cleavage between the nitrogen atom in the sulfonamide group and the pyrimidine ring occurred.

The third initial reaction is the direct substitution of the sulfonamide group with a hydroxyl group and the resulting formation of *p*-AP. Mentioned above, the formation of *p*-AP has never been reported in previous studies. The hydroxylation of the aromatic ring is the major initial reaction, however, once hydroxylation of phenyl ring in SMT occurred, hydroxyl group may be introduced into the *o*- or *m*-position from the amino group. If sequential cleavage of sulfonamide bond and desulfonation occur, *o*- or *m*-AP may form instead of *p*-AP. Therefore direct substitution of the sulfonamide group must occur at initial stage for the formation of *p*-AP. Such a hydroxyl group substitution was reported by Zhang et al. in the photocatalytic decomposition of acetaminophen, hydroquinone directly formed from acetaminophen (Zhang et al., 2008). Moreover, we insist on this reaction because *p*-AP formed at initial stage of SMT photocatalytic decomposition. *p*-AP was also observed at the initial stage of the photocatalytic decomposition of SA, suggesting that direct substitution by a hydroxyl group may occur. The maximum concentration of *p*-AP observed during SMT decomposition was 1.4 μM after 20-min treatment, determined using a standard. Based on the initial concentration of SMT (36.0 μM), stoichiometrically 3.9% of the SMT appeared to be converted to *p*-AP. TiO_2 photocatalysis in aqueous media often yields many intermediates owing to irregular and uncontrollable radical reactions. In our previous study, the amount of intermediates formed during the photocatalytic decomposition of bisphenol A were quantified and the highest yield of first intermediates was found to be 7.0% based on the amount of parent compound (Fukahori et al., 2003). From these results, it is plausible that *p*-AP is the first intermediate formed from SMT and direct substitution of the sulfonamide group with a hydroxyl group is one of the major initial reactions during the photocatalytic decomposition of SMT.

4. Conclusion

The photodegradation behavior of SMT using TiO_2 was investigated. The time courses of SMT and ion concentrations and NPOC indicated the complete mineralization and photocatalytic degradation of SMT. In addition, the structures of the intermediates formed during the photocatalytic decomposition of SMT, SA, and ADMP were analyzed using LC/MS/MS. Seven intermediates were

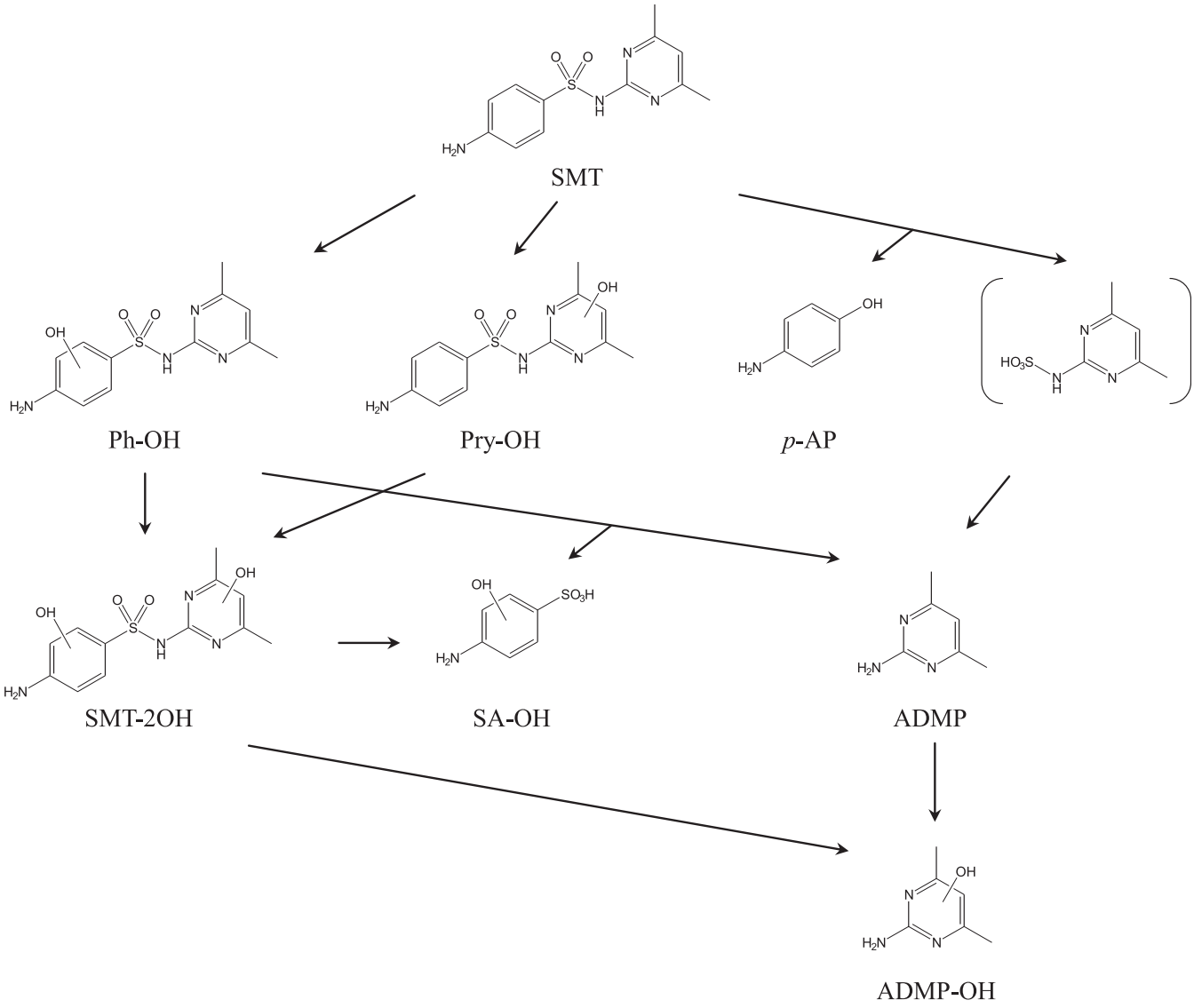

Fig. 7. Proposed photocatalytic decomposition pathway of SMT.

deduced from the estimated molecular weight and fragment patterns. Among them, the formation and accumulation of *p*-AP at the initial stage of SMT decomposition was an important clue for novel reaction pathway. Three initial reactions were suggested from the formation behaviors of the intermediates; the hydroxylation of phenyl and the pyrimidine ring, and direct substitution of the sulfonamide group with a hydroxyl group.

Acknowledgment

This work was financially supported by the Core Research for Evolutional Science and Technology (CREST) program of the Japan Science and Technology Agency.

References

Abellán, M.N., Bayarri, B., Giménez, J., Costa, J., 2007. Photocatalytic degradation of sulfamethoxazole in aqueous suspension of TiO_2. Appl. Catal. B: Environ. 74, 233–241.

Baran, W., Adamek, E., Sobczak, A., Makowski, A., 2009. Photocatalytic degradation of sulfa drugs with TiO_2, Fe salts and TiO_2/$FeCl_3$ in aquatic environment -Kinetics and degradation pathway. Appl. Catal. B: Environ. 90, 515–525.

Bendz, D., Paxéus, N.A., Ginn, T.R., Loge, F.J., 2005. Occurrence and fate of pharmaceutically active compounds in the environment, a case study: Höje River in Sweden. J. Hazard. Mater. 122, 195–204.

Panel on Animal Health, Food Safety, and Public Health, National Research Council Committee on Drug Use in Food Animals, 1999. The Use of Drugs in Food Animals: Benefits and Risks. National Academy Press, Washington, DC.

Fent, K., Weston, A.A., Caminada, D., 2006. Ecotoxicology of human pharmaceuticals. Aquat. Toxicol. 76, 122–159.

Fukahori, S., Ichiura, H., Kitaoka, T., Tanaka, H., 2003. Capturing of bisphenol A photodecomposition intermediates by composite TiO_2-zeolite sheets. Appl. Catal. B: Environ. 46, 453–462.

Fukahori, S., Fujiwara, T., Ito, R., Funamizu, N., 2012. Photocatalytic decomposition of crotamiton over aqueous TiO_2 suspensions: determination of intermediates and the reaction pathway. Chemosphere 89, 213–220.

Heberer, T., 2002. Occurrence, fate, and removal of pharmaceutical residues in the aquatic environment: a review of recent research data. Toxicol. Lett. 131, 5–17.

Hernando, M.D., Mezcua, M., Fernández-Alba, A.R., Barceló, D., 2006. Environmental risk assessment of pharmaceutical residues in wastewater effluents, surface waters and sediments. Talanta 69, 334–342.

Hu, L., Flanders, P.M., Miller, P.L., Strathmann, T.J., 2007. Oxidation of sulfamethoxazole and related antimicrobial agents by TiO_2 photocatalysis. Water Res. 41, 2612–2626.

Ito, M., Fukahori, S., Fujiwara, T., 2013. Adsorptive removal and photocatalytic decomposition of sulfamethazine in secondary effluent using TiO_2-zeolite composites. Environ. Sci. Pollut. R. 21, 834–842.

Kaniou, S., Pitarakis, K., Barlagianni, I., Poulios, I., 2005. Photocatalytic oxidation of sulfamethazine. Chemosphere 60, 372–380.

Kim, I., Yamashita, N., Tanaka, H., 2009. Performance of UV and UV/H_2O_2 processes for the removal of pharmaceuticals detected in secondary effluent of a sewage treatment plant in Japan. J. Hazard. Mater. 166, 1134–1140.
Ternes, T.A., Stüber, J., Herrmann, N., McDowell, D., Ried, A., Kampmann, M., Teiser, B., 2003. Ozonation: a tool for removal of pharmaceuticals, contrast media and musk fragrances from wastewater? Water Res. 37, 1976–1982.
Vulliet, E., Emmelin, C., Chovelon, J., Guillard, C., Herrmann, J., 2002. Photocatalytic degradation of sulfonylurea herbicides in aqueous TiO_2. Appl. Catal. B: Environ. 38, 127–137.
Yang, H., Li, G., An, T., Gao, Y., Fu, J., 2010. Photocatalytic degradation kinetics and mechanism of environmental pharmaceuticals in aqueous suspension of TiO_2: a case of sulfa drugs. Catal. Today 153, 200–207.
Zhang, X., Wu, F., Wu, X.W., Chen, P., Deng, N., 2008. Photodegradation of acetaminophen in TiO_2 suspended solution. J. Hazard. Mater. 157, 300–307.